Abstract

We investigate the application of mesoscopic response functions (MRFs) to characterise a large set of networks of fungi and slime moulds grown under a wide variety of different experimental treatments, including inter-species competition and attack by fungivores. We construct "structural networks" by estimating cord conductances (which yield edge weights) from the experimental data, and we construct "functional networks" by calculating edge weights based on how much nutrient traffic is predicted to occur on each edge. Both types of networks have the same topology, and we compute MRFs for both families of networks to illustrate two different ways of constructing taxonomies to group the biological networks into related clusters. Although both network taxonomies generate intuitively sensible groupings of networks across species, treatments, and laboratories, we find that clustering using the functional-network measure appears to give more parsimonious groups. We argue that MRFs provide a useful quantitative measures of network behaviour that can help to summarise an expanding set of increasingly complex experimental biological networks and to present the information in an accessible form.

END NOTE
Mesoscale Analyses of Fungal Networks

Sang Hoon Lee
Integrated Energy Center for Fostering Global Creative Researcher (BK 21 plus) and
Department of Energy Science, Sungkyunkwan University, Suwon 440–746, Korea
Oxford Centre for Industrial and Applied Mathematics, Mathematical Institute,
University of Oxford, Oxford OX2 6GG, United Kingdom

Mark D. Fricker
Department of Plant Sciences, University of Oxford, South Parks Road, Oxford OX1
3RB, United Kingdom
CABDyN Complexity Centre, University of Oxford, Oxford OX1 1HP, United Kingdom

Mason A. Porter
Oxford Centre for Industrial and Applied Mathematics, Mathematical Institute,
University of Oxford, Oxford OX2 6GG, United Kingdom
CABDyN Complexity Centre, University of Oxford, Oxford OX1 1HP, United Kingdom

Fungi are unusual multi-cellular macroscopic organisms: their entire growth form is a living network of interconnected microscopic tubular cells (termed "hyphae") that can branch, fuse, or aggregate to form larger, visible structures (termed "cords"). The resulting mycelial network has to transport nutrients from sites of acquisition to the growing tips to fuel further exploration for new resources that exist with an unknown distribution in a fluctuating, patchy, and competitive environment (Heaton *et al.*, 2012). Additionally, mycelial networks provide food for small grazing invertebrates, and they thus suffer continuous attack and damage (Crowther *et al.*, 2012). Although most growth is out of sight in the soil and leaf litter, this belies the essential role that fungi play in critical ecosystem services, such as decomposition of organic matter and mineral nutrient recycling. Furthermore, the influence of climate change, seasonal temperature shifts, and anthropogenic inputs are all likely to have an impact on network organisation, foraging success, and outcome of multi-species competitive interactions (A'Bear *et al.*, 2013a; A'Bear *et al.*, 2013b; Boddy *et al.*, 2014).

Because fungi do not have a centralised system to coordinate development, one can posit from the diversity of recognisable network patterns that each fungal species uses a (slightly) different set of local rules to continuously balance investment in growth, transport efficiency, and resilience that collectively maximise the long-term global success of the organism. However, unlike most species, fungi have a highly plastic morphology with few quantifiable traits. Thus, to date, most descriptions of fungal behaviour have relied on relatively simple growth measures, coupled with qualitative descriptors, with no detailed evaluation of subtle changes in growth form and network organisation. Constructing taxonomies of fungal networks thus has the potential to provide insights into adaptive fungal

behaviour and to help elucidate the similarities and differences among the underlying rules that govern behaviour. As a fungus is essentially a living network, we describe the change in fungal network architecture as *network behaviour*.

It is also relevant to compare fungal networks to the acellular slime mould, *Physarum polycephalum*, which is a second type of network-forming organism and which is taxonomically very distinct from fungi. The acellular slime mould is essentially a single giant multi-nucleate animal cell. One can grow fungi and slime moulds in laboratories, and it is consequently possible to expose them to a wide variety of experimental conditions and species interactions, in multiple replicates, to generate a rich collection of networks for analysis. Therefore, investigating such adaptive, self-organised networks — which are honed by evolution — provides a fascinating opportunity to uncover underlying principles of network organisation in a biological context, evaluate the relevance of network descriptors that have been developed in related disciplines to evolved network behaviour, and explore how much utility biologically-inspired algorithms have in other domains (Fricker *et al.*, 2009; Tero *et al.*, 2010; Kunita *et al.*, 2013).

In Fig. 1, we show time series of fungal growth for one species (*Resinicium bicolor*) that tends to grow as a relatively sparse network [panel (A)] and a second species (*Phanerochaete velutina*) that forms more cross-links. For the latter, we illustrate the impact of increasingly complex microcosms for which the level and positioning of resources are both varied [panels (B) and (C)], resources become depleted and the networks shrink, in both the presence and the absence of attack by mycophagous insects [panels (D) and (E)], and networks are grown in competition with another species (*Hypholoma fasciculare*) both with and without predation [panels (F) and (G)]. The variety of examples in Fig. 1 gives a visual indication of the challenges facing biologists when trying to describe the variation in network organisation, as the structural changes in these different scenarios can be rather subtle.

We have just discussed network architecture, but we are also interested in the function of the network in long-distance nutrient transport from sources (wood blocks) to sinks (growing hyphae at the foraging margin). In Fig. 2, we show a network formed by *Phanerochaete velutina* growing from five wood-block inocula that are placed in a pentagonal arrangement on a compressed black-sand substrate, in a similar arrangement to Fig. 1(C). The network emerges [panel (A)] as cords fuse and are strengthened, or are recycled and disappear. One can map functional flows in the network using radiotracers [panel (B)] to provide a snapshot of nutrient transport [panel (C)]. One can extract the network architecture using image analysis and determine edge weights according to conductance (Onnela *et al.*, 2012; Bebber *et al.*, 2007; Heaton *et al.*, 2012) to give a "structural network" [panel (D)] or according to "path score" (PS) that indicates edge importance (Lee *et al.*, 2014) to estimate a "functional network" [panel (E)]. (See Sec. S1 in the Supplementary Text and Table for the detailed definitions of the two types of networks.) Using either of the networks, one generate three mesoscopic response functions [MRFs; panel (F)] (Onnela *et al.*, 2012) to examine network "community structure" at multiple scales. In Fig. 3, we show the resulting taxonomy for 270 fungal networks based on structure [panel (A)] and function [panel (B)]. For more details on data and analyses, see the Supplementary Text and Table. We also include the data for all networks as Supplementary Material.

In both the structural and functional networks, the complexity of the wide range of experimental conditions is reduced to a set of intuitively sensible clusters. We also observe that the "functional" PS measure provides more harmonious groupings, which are clustered by species, substrate, resource level, grazing, and interaction. We also observe that networks that arise from some treatments are spread across the taxonomy. In particular, as large networks of *Phanerochaete velutina* deplete their resources, they move from clusters with well cross-linked networks to very sparse networks, similar to the normal growth pattern of *Resinicium bicolor*.

Supplementary Material

We provide detailed descriptions of data, methodology, and results as Supplementary Text and Table. We include the entire set of 270 networks as additional Supplementary Material in the file `fungal_networks_MATLAB.zip`, which includes the sparse adjacency matrices (denoted as `A`) and the coordinate matrices (the first and second columns represent horizontal and vertical coordinates, respectively) of the node (denoted as `coordinates`) in MATLAB format. We use the codes in Table S1 in the Supplementary Text and Table to name the files, and the folders `Conductance` and `PathScore`, respectively, contain the conductance-based and PS-based edge weights. We also provide the complete list of fungal networks as a spreadsheet file (`list_of_fungal_networks.xlsx`) in Microsoft EXCEL format.

Acknowledgements

SHL and MAP acknowledge a grant from the EPSRC (EP/J001759/1). SHL was supported by Basic Science Research Program through the National Research Foundation of Korea (NRF) funded by the Ministry of Education (2013R1A1A2011947). MDF acknowledges grant RGP0053/2012 from Human Frontiers of Science Program. We thank M. Anantharaman, D. Leach, S. Kala, G. Tordoff for collecting images and networks that have not yet been published. The MRF source code is available at `http://www.jponnela.com/web_documents/mrf_code.zip`.

References

A'Bear, A. D., Jones, T. H., & Boddy, L. (2013a). Potential impacts of climate change on interactions among saprotrophic cord-forming fungal mycelia and grazing soil invertebrates. *Fungal Ecology*, **10**, 34–43.

A'Bear, A. D., Murray, W., Webb, R., Boddy, L., & Jones, T. H. (2013b). Contrasting effects of elevated temperature and invertebrate grazing regulate multispecies interactions between decomposer fungi. *PLOS ONE*, **8**, e77610.

Bebber, D., Hynes, J., Darrah, P. R., Boddy, L., & Fricker, M. D. (2007). Biological solutions to transport network design. *Proceedings of the Royal Society B: Biological Sciences*, **274**, 2307–2315.

Boddy, L., Büntgen, U., Egli, S., Gange, A. C., Heegaard, E., Kirk, P. M., Mohammad, A., & Kauserud, H. (2014). Climate variation effects on fungal fruiting *Fungal Ecology*, **10**, 20–33.

Crowther, T. W., Boddy, L., & Jones, T. H. (2012). Functional and ecological consequences of saprotrophic fungus-grazer interactions. *The ISME Journal*, **6**, 1992–2001.

Fricker, M. D., Boddy, L., Nakagaki, T., & Bebber, D. P. (2009). Adaptive biological networks. In Gross T. & Sayama H. (Eds.), *Adaptive networks: theory, models and applications* (pp. 51–70). Springer, New York, United States.

Heaton, L. L. M., López, E., Maini P. K., Fricker M. D., & Jones, N. S. (2010). Growth-induced mass flows in fungal networks. *Proceedings of the Royal Society B: Biological Sciences*, **277**, 3265–3270.

Heaton, L. L. M., Obara, B., Grau, V., Jones, N. S., Nakagaki, T., Boddy, L., & Fricker, M. D. (2012). Analysis of fungal networks. *Fungal Biology Reviews*, **26**, 12–29.

Kunita, I., Yoshihara, K., Tero, A., Ito, K., Lee, C.-F., Fricker, M. D., & Nakagaki, T. (2013). Adaptive path-finding and transport network formation by the amoeba-like organism physarum. In *Proceedings in Information and Communications Technology*, **6**, 14–29. Springer, New York, United States.

Lee, S. H., Cucuringu, M., & Porter, M. A. (2014). Density-based and transport-based core-periphery structures in networks. *Physical Review E*, **89**, 032810.

Newman, M. E. J. (2010). *Networks: an introduction* (Oxford University Press, UK).

Onnela, J.-P., Fenn, D. J., Reid, S., Porter, M. A., Mucha, P. J., Fricker, M. D., & Jones, N. S. (2012). Taxonomies of networks from community structure. *Physical Review E*, **86**, 036104.

Tero, A., Takagi, S., Saigusa, T., Ito, K., Bebber, D. P., Fricker, M. D., Yumiki, K., Kobayashi, R., & Nakagaki, T. (2010). Rules for biologically inspired adaptive network design. *Science*, **327**, 439–442.

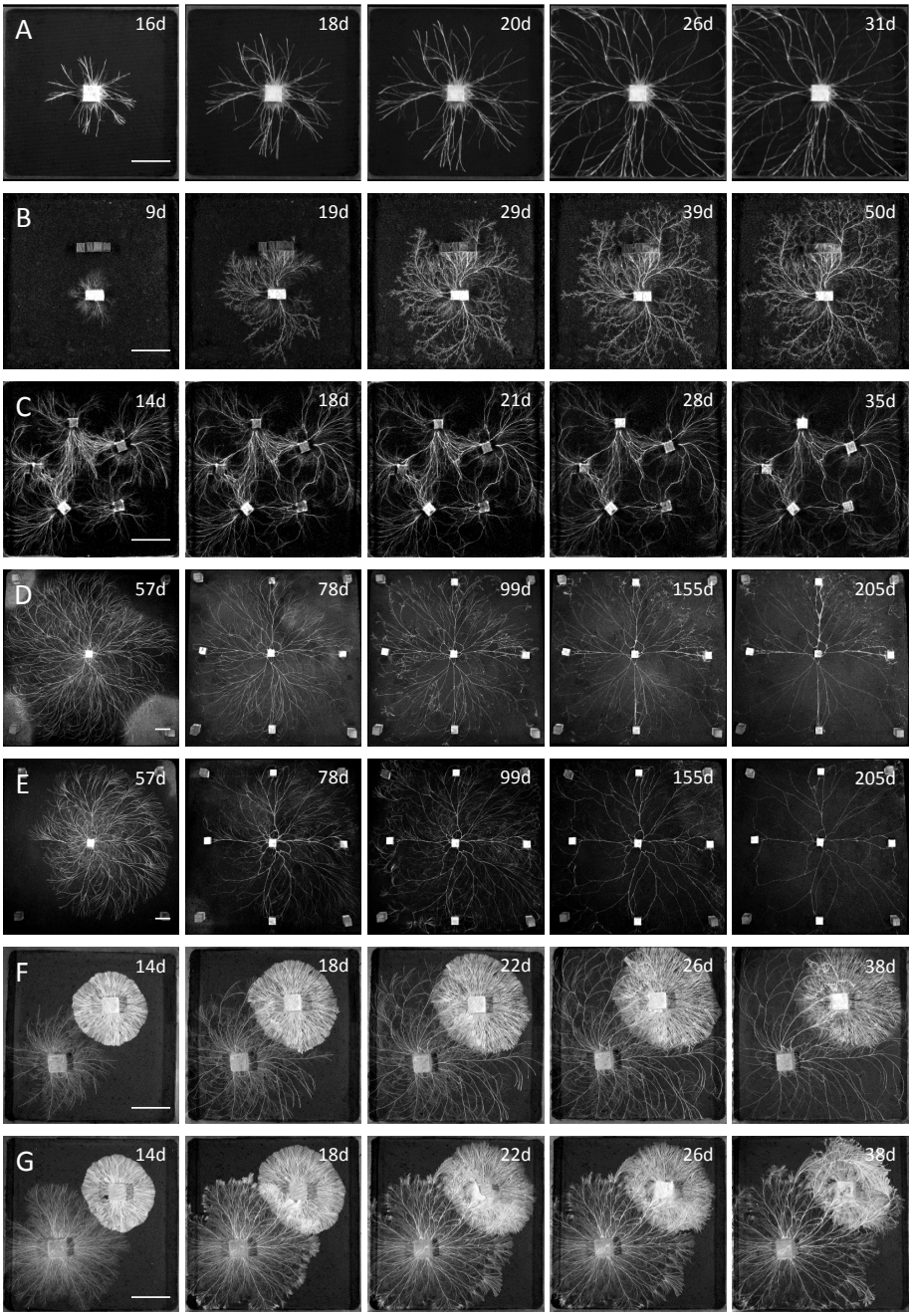

Fig. 1. (A) Growth of *Resinicium bicolor* on soil as a relatively sparse network. (B) Growth of *Phanerochaete velutina* on black sand with an additional set of four wood-block resources. (C) Network formation in *Phanerochaete velutina* over 30 days on a compressed black-sand substrate from a pentagonal arrangement of wood-block inocula. (D) Large microcosm (57 mm × 57 mm) of *Phanerochaete velutina* supplemented with four additional resources. The network begins to regress as it consumes the resources. (E) Similar experimental microscosm to (D), except that grazing insects were added on day 49. (F) *Phanerochaete velutina* growing in competition with *Hypholoma fasciculare*. (G) *Phanerochaete velutina* growing in competition with *Hypholoma fasciculare* in the presence of grazing insects. [Each scale bar (see the left panels) represents 50 mm, and the upper right corner of each panel gives the amount of time in days.]

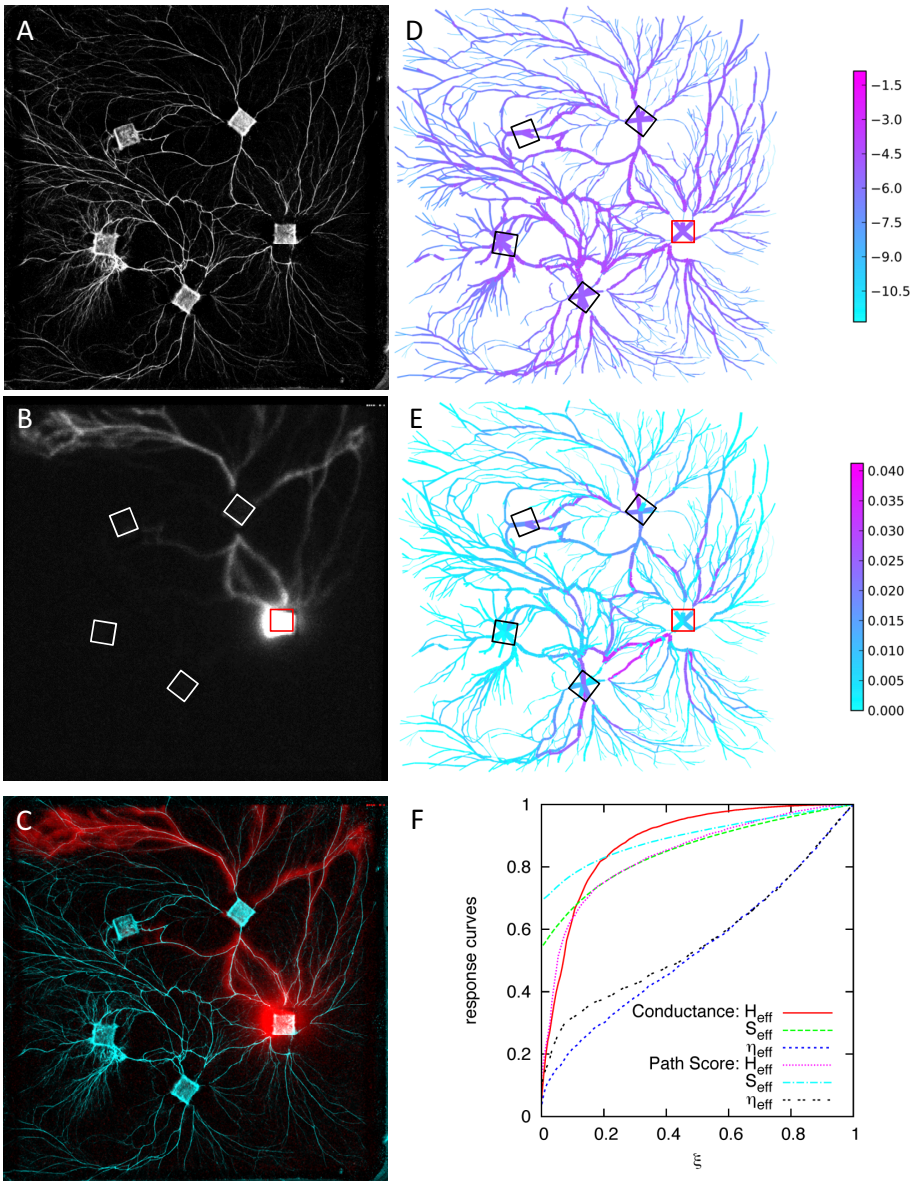

Fig. 2. (A) One of the fungal networks formed by *Phanerochaete velutina* after 30 days of growth across a compressed black-sand substrate from a pentagonal arrangement of wood-block inocula. (B) Path of radiolabeled nutrient (^{14}C-amino-isobutyrate) added at 30 days and imaged using photon-counting scintillation imaging for 12 hours. (C) Merged overlay of panels (A) and (B) to highlight the path that is followed by the radiolabel. (D) We colour the edges of the manually-digitised network according to the logarithm of the conductance values. Edge thickness represents cord thickness. (E) We colour the edges according to the path score (PS) values of the fungal network. (F) MRF curves for conductance-based and PS-based weights. We show MRF curves for effective energy H_{eff}, effective entropy S_{eff}, and effective number of communities η_{eff}. See (Onnela *et al.*, 2012) for details on MRFs, and note that the energy is proportional to the negative of optimised modularity. For the MRF analysis, we remove nodes with degree $k = 2$, and we adjust the weights of the edges that connect the remaining nodes to include the values for each $k = 2$ segment. [The edges in panels (D) and (E) include nodes with degree 2, as they are needed to trace the curvature of the cords.]

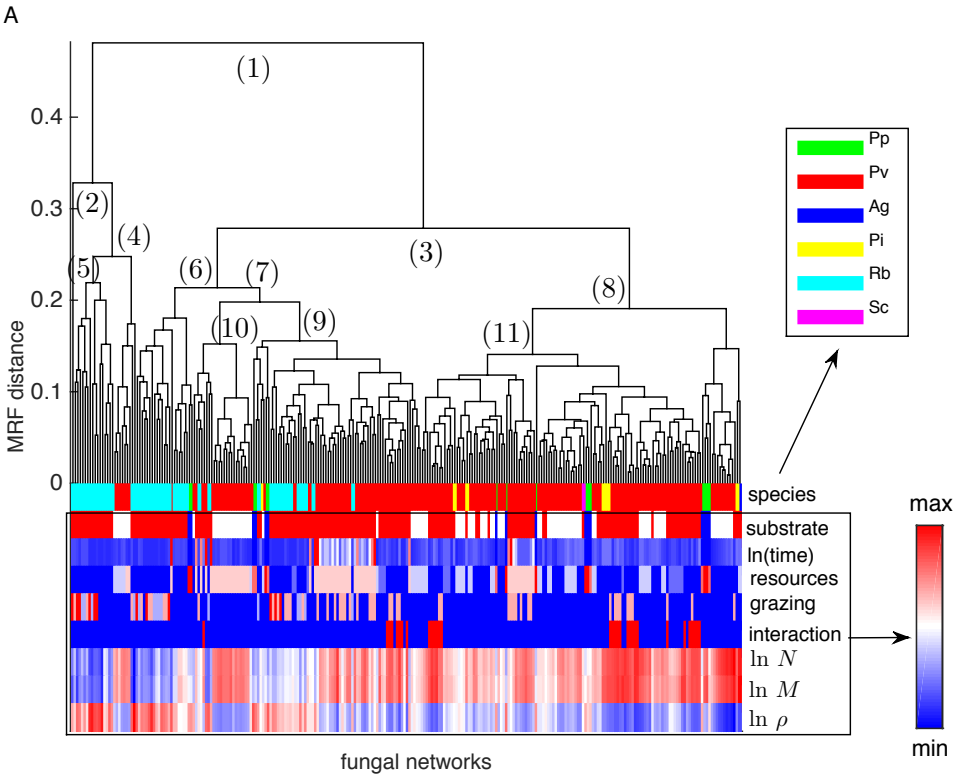

Fig. 3. Taxonomies of 270 fungal (and slime-mould) networks determined using (A) conductance G and (B) (next page) PS values (Lee *et al.*, 2014) as the edge weights. We produced the dendrogram that represents this taxonomy using an MRF analysis (Onnela *et al.*, 2012), where we applied average linkage clustering (Newman, 2010) to the MRF-distance from principal component analysis of the three different MRFs (effective energy, effective energy, and effective number of communities) (Onnela *et al.*, 2012). We used the same methodology (including the determination of community structure using modularity optimisation with a resolution parameter) as in (Onnela *et al.*, 2012). See Table S1 in the Supplementary Text and Table for the species abbreviations; the levels of substrate, resources, and grazing; and a discussion of the numbered branching points. At the bottom of the taxonomies, we also show the logarithms of number of nodes N, number of edges M, and the edge density $\rho = 2M/[N(N-1)]$. We label the main branch points in each dendrogram in parentheses. (Note that "branches" in a fungal network are different from "branches" in a taxonomy. It is standard to use such terminology in both contexts.)

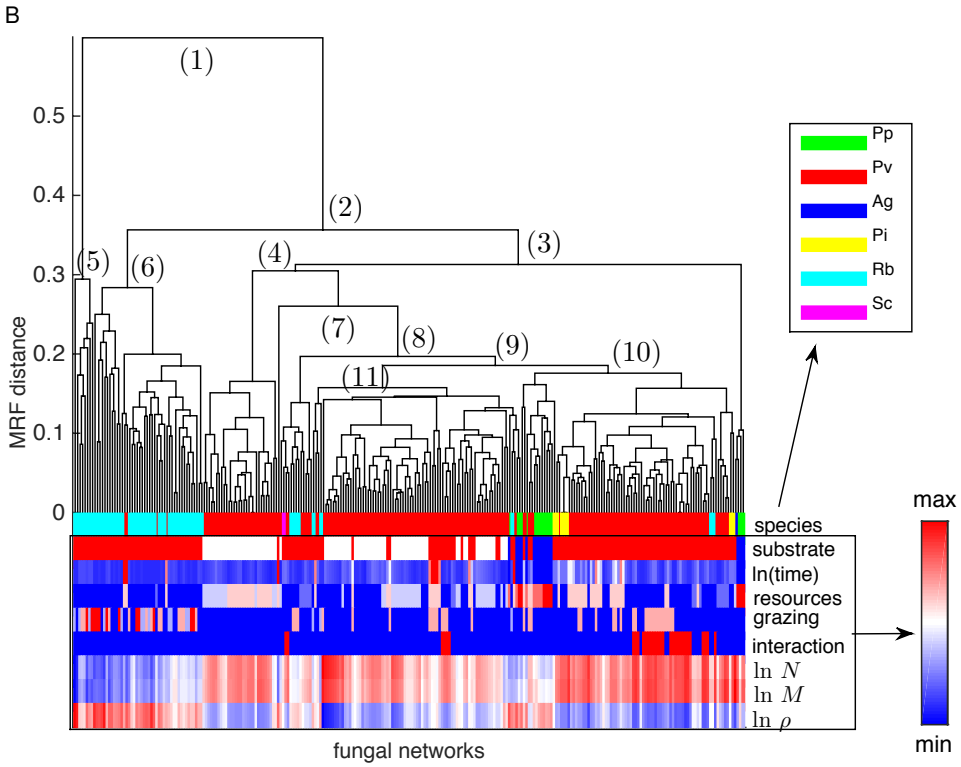
B
MRF distance
0
0.1
0.2
0.3
0.4
0.5
(1)
(2)
(3)
(4)
(5)
(6)
(7)
(8)
(9)
(10)
(11)
Pp
Pv
Ag
Pi
Rb
Sc
species
substrate
ln(time)
resources
grazing
interaction
ln N
ln M
ln ρ
max
min
fungal networks

Supplementary Text and Table for END NOTE *Mesoscale Analyses of Fungal Networks*

Sang Hoon Lee,[1,2] Mark D. Fricker,[3,4] and Mason A. Porter[2,4]

[1]*Integrated Energy Center for Fostering Global Creative Researcher (BK 21 plus) and Department of Energy Science, Sungkyunkwan University, Suwon 440–746, Korea*
[2]*Oxford Centre for Industrial and Applied Mathematics, Mathematical Institute, University of Oxford, OX2 6GG, United Kingdom*
[3]*Department of Plant Sciences, University of Oxford, South Parks Road, Oxford OX1 3RB, United Kingdom*
[4]*CABDyN Complexity Centre, University of Oxford, Oxford OX1 1HP, United Kingdom*

S1. DATA AND METHODS

To make progress in the study of fungal networks, it is important to develop tools to characterise their structure, their function, and how they develop over time and using different treatments. There is a long history of qualitative description of fungal networks that dates back to the seminal work of Buller in the 1930s (see, e.g., [3]). More recently, network characterisations have been based on translating a mycelial image to a planar, weighted, undirected graph [1, 6, 8]. In such characterisations, the nodes are located at hyphal tips, branch points, and anastomoses (i.e., hyphal fusions). The edges represent cords, and their weights are determined from the Euclidean length (L) and radius (r) of each cord combined either as (1) the cylindrical volume $V = \pi r^2 L$ to represent the biological "cost" of the cord or (2) the predicted conductance $G = r^2/L$. The conductance assumes that the cords are bundles of equally-sized vessels, so that the aggregate conductance scales with the cross-sectional area of the whole cord (rather than a single vessel, in which case the conductance would scale with r^4 for Pouiseille flow).[1]

In the present paper, we refer to the above network representations as *structural networks*. Simple network measures, such as notions of meshedness (for planar networks), clustering coefficients, and betweenness centrality, have been calculated from graph representations of fungal networks [1]. However, the computation of simple diagnostics has not been able to capture the subtle differences in spatial structure between species or in the same species when they are responding to different experimental conditions [8]. Although such features are hard to describe quantitatively, human observers can see them qualitatively.

Detailed measurements and modelling have been used to experimentally define development of network architecture over time, predict the flow of water and nutrients through the resulting empirical network using an advection and diffusion model, and compare model output with experimentally measured radiolabel distributions used to track the actual nutrient movement [7, 8]. Although such an approach has revealed good correlations between growth-induced fluid flows and nutrient transport, and one can even see hints of the local rules that optimise behaviour, it is too technically demanding and costly to be used as a routine analysis of network behaviour across multiple data sets. Other approaches are thus necessary to compare the structures and function of a large set of fungal species or the same species over time and in different experimental conditions.

In a recent paper [15], two of us (and our coauthors) illustrated that examining community structure of fungal networks using a mesoscopic response function (MRF) provides biologically-sensible clusterings of different species and developmental stages for a particular species. In the present paper, we explore the utility of such community-based classification using a much larger set of fungal networks that includes a wide variety of different developmental stages, nutrient regimes, growth substrates, competition, and levels of predation. We also examine the difference in classification based on a structural view of such networks that uses only the predicted conductance G of each cord to one that is based on a predicted functional view of the importance of each cord for transport. For the latter, we calculate the weight of each cord using a "path score", which is a diagnostic (see the definition below) that measures the importance of an edge for transport of nutrients in a network in a way that is more nuanced than standard measures of betweenness centrality [12].

The computation of path scores also highlights core-periphery structures in fungal networks that are based on transport properties rather than on the usual density-based notions of such structures [4]. In a fungal (or slime-mould) network, we expect core cords to highlight the dense parts of the network near the inoculum (i.e., source material for a new culture) or in parts that connect to additional resources, whereas the periphery could correspond to the foraging margin. Transport-based measures of core-periphery structure for both nodes and edges in networks were recently investigated in a wide variety of networks and using different transportation strategies (e.g., both geodesics and random walks) [12]. (See [13] for related theoretical work.) Because one of the primary predicted functions of fungal networks is nutrient transport, it is more appropriate to examine core versus peripheral edges (i.e., cords) rather than nodes.

As discussed in [12], we quantify a transport-based measure of "coreness" called the *path score* (PS) for each edge by examining which cords appear most often on "backup paths" if any particular cord is broken. This measure thereby incorporates elements of both betweenness centrality and network

[1] Note that [15] used the cylindrical volume $V = \pi r^2 L$ for the edge weights in fungal networks, although the authors of that paper mistakenly wrote that they used conductance.

resilience. We expect that core edges in a network should occur more frequently than peripheral edges in short backup paths. One can define path scores for both directed and undirected networks and for both weighted and unweighted networks. We treat the networks that we construct from our fungal systems as weighted and undirected.

We denote the set of edges by $\mathbb{E} = \{(j,k)|$ node j is adjacent to node $k\}$ and the number of edges by $M = |\mathbb{E}|$. The PS for edge e is defined by

$$\mathrm{PS}(e) = \frac{1}{M} \sum_{(j,k)\in\mathbb{E}} \sum_{\{p_{jk}\}} \sigma_{jek}[\mathbb{E} \setminus (j,k)] \,, \tag{S1}$$

where $\sigma_{jek}[\mathbb{E} \setminus (j,k)] = 1/|\{p_{jk}\}|$ if edge e is in the set $\{p_{jk}\}$ that consists of "optimal backup paths" from node j to node k (where we stress that the edge (j,k) is removed from $\mathbb{E}$) and $\sigma_{jek}[\mathbb{E} \setminus (j,k)] = 0$ otherwise. Note that a notion of coreness based on the response to node removal was used in [19] in the context of closeness centrality rather than betweenness centrality.

To determine an optimal path between nodes i and j, we find the backup path $p_b(ij)$ that consists of the set of connected edges between i and j that minimises the sum of the resistances, $\sum_{(k,l)\in p_b(ij)} R_{kl}$, for all edges (k,l) of the network in which the edge $e_{ij} := (i,j)$ has been removed. The resistance of edge (k,l) is $R_{kl} = 1/G_{kl}$, where the conductance is $G_{kl} = r^2/L$, the quantity r is the radius of a cord, and L is the length of edge (k,l). We set $R_{kl} = 0$ (instead of $R_{kl} = \infty$) when an edge is removed because the edge simply does not exist. To capture a functional view of the fungal networks (i.e., to obtain so-called *functional networks*), we also construct weighted networks in which we preserve topology but use PS values instead of conductance values as the edge weights.

In Fig. 2 of the main text, we show a network formed by *Phanerochaete velutina* growing from five wood-block inocula that are placed in a pentagonal arrangement on a compressed black-sand substrate. The fungal network that forms has a relatively densely interconnected core and relatively tree-like foraging branches on the periphery. Adding a radiolabel to one of the wood blocks and subsequently doing photon-counting scintillation imaging (PCSI) provides a snapshot of how nutrients are transported at that particular instant through some of the core cords to a second wood block and then outwards to part of the network periphery. The PS values on the edges of a fungal network reflect the actual movement path in the region of the colony in which radiolabel was translocated, suggesting that the PS values capture some aspects of real nutrient movement in fungal networks. However, there is not a simple correspondence between PS values and observed nutrient transport, as there are cords with high PS values that could have been utilised to reach the neighbouring wood block on the left even though there is no detectable radiolabel translocation over the 12-hour time period of the measurement.

S2. RESULTS AND DISCUSSION

To compare the properties of the various structural and functional networks, we produce a taxonomy of the fungal networks from MRFs of each network [15] that highlight mesoscale "community structure" [5, 16]. In network terms, communities are densely connected internally, and there are sparse connections between communities relative to a null model. To identify community structure, we optimise a multiresolution version of the modularity quality function. We use the Newman–Girvan null model augmented by a resolution parameter and examine communities of different size scales by tuning that parameter [14, 17]. For each network, we obtain curves for several scaled quantities (number of communities, modularity, and entropy) as a function of the resolution parameter. These diagnostics yield a mesoscale fingerprint for each network. Two networks are close to each other in the taxonomy if their MRF curves have similar shapes to each other. (See [15] for details.) We thereby construct two taxonomies — one for the structural networks and another for the functional networks — that give a pair of "family trees" that describe how closely the various networks are related in the form of a dendrogram.

In Fig. 3 of the main text, we show the resulting dendrograms for 270 fungal networks based on structure and function. (We include the data for all networks as Supplementary Material.) Recall that the structural and functional networks have the same topologies, but their edge weights are different: the weights are given by estimated conductance values for the structural networks and by PS values for the functional networks. For both the structural and functional fungal networks, the simplest network measures for each leaf (e.g., number of nodes, number of edges, and node density) only reveal a limited correlation with the major branches in the dendrogram. This suggests that the classification is not trivially dominated by the size of each network and also that it is necessary to go beyond the computation of only such simple measures to produce a reasonable taxonomy. When we code leaves according to the values of the major attributes in each experiment (species, substrate, time point, resource level, and grazing intensity), we observe that groups with similar attributes begin to emerge and are visible as substantial contiguous blocks in the dendrograms. Nevertheless, we also observe that each attribute is not uniquely associated with one group, which suggests that the classifications are again not a trivial separation by any one of these attributes (e.g., species) alone. This suggests, in particular, that they also reflect similarity in the topologies and weights (i.e., geometries) of the networks.

The Pearson correlation coefficient between the MRF distance values (see Appendix B 2 of [15]) for the structural and functional network sets is 0.418. (The p-value is less than 10^{-308}, which is the minimum value of floating-point variables in Python.) In contrast, the mean correlation coefficient from 100 uniform-at-random permutations of the MRF distance values is 2.12×10^{-5}, with a standard deviation 3.67×10^{-3}. We infer that there is some degree of correlation between the weights in the structural and functional networks, although they clearly capture different properties of the fungi.

Supplementary Table S1: Species and experimental conditions used in Fig. 3 of the main text.

Attribute	Code/Level (Colour)	Descriptions
Species	*Pp*	*Physarum polycephalum*: an acellular slime mould that forms networks but is taxonomically distinct from fungi
	Pv	*Phanerochaete velutina*: a foraging saprotrophic woodland fungus that forms reasonably dense networks
	Ag	*Agrocybe gibberosa*: a foraging saprotrophic fungus that is isolated from garden compost and forms dense networks
	Pi	*Phallus impudicus*: forms regular, highly cross-linked networks but grows relatively slowly
	Rb	*Resinicium bicolor*: forages rapidly with a sparse network that is not very cross-linked
	Sc	*Strophularia caerulea*: a foraging saprotrophic woodland fungus that is isolated from birch woodland and forms dense networks
resources	I/min (blue)	Inoculum only
	I+R/level 1	Initial colonised wood block (inoculum, I) plus a single additional wood-block resource (R)
	I+4 × R/level 2	Inoculum plus four additional wood-block resources (positioned as a cross)
	I+4 × R/level 2	Inoculum plus four wood-block resources placed together
	5 × I/level 3	Five inocula placed in a pentagonal arrangement
	Tokyo/level 4	Pattern of oat flakes placed to match the major cities around Tokyo
	UK/max (red)	Pattern of oat flakes placed to match the major cities in the UK
grazing	U/min (blue)	Ungrazed
	Fc/level 1	*Folsomia candida*: a small soil arthropod that grazes on fungal networks with low density (10 per microcosm) [18]
	Fc or *Fc*-M/level 2	*Fc* with medium density (20 per microcosm)
	Fc-H/max (red)	*Fc* with high density (40 per microcosm)
substrate	A/blue	Agar: used as a growth medium (substrate) for *Physarum polycephalum*
	B/white	Black sand: a nutrient-free substrate used for radiolabel-imaging experiments
	S/red	Compressed, non-sterile soil that closely represents the natural growth environment for the fungi
interaction	N/blue	no interaction: fungal species grown on its own
	Hf/red	competition with *Hypholoma fasciculare*

A key challenge is to try to interpret the taxonomic groupings from a biological perspective to obtain insights that cannot be captured from qualitative descriptions of each network, particularly when making comparisons between different experiments from different laboratories over an extended time period. To do this, we follow the major branch points of the dendrograms in a top-down analysis of each taxonomy. We label branches in the dendrograms in the order in which they occur in the taxonomic hierarchies. In the conductance-based classification [see Fig. 3(A) of the main text], a small group splits off at a high level (1, 2). This group then separates into two parts: one contains *Resinicium bicolor* (*Rb*) with some grazing (5), and the other has *Phanerochaete velutina* (*Pv*) grown on black sand (4). The other main branch splits to give two clusters (3), but the underlying rationale is not immediately obvious, as both parts include a mixture of different conditions of the attributes (see Table S1). The clearest subsequent groupings emerge as clusters of *Rb* with grazing at earlier time points (6, 9) and *Pv* on black sand with high resources (10).

Following the same top-down approach on the PS-based taxonomy [see Fig. 3(B) of the main text] provides groupings that are easier to interpret than the ones from the conductance-based taxonomy. The first set of high-level branch points (1, 2, 5, and 6) all separate clades of *Rb*, where subsequent divisions reflect the level of grazing. Branch point (4) separates a group of *Pv* on black sand with relatively high levels of resource, and branch point (7) yields a single *Pv* network from one of the large, shrinking network sequences. Interestingly, these networks are interspersed across the whole dendrogram. (See the isolated pink and red bars in the "ln(time)" bar.) During development, these large networks initially cluster with other well-connected networks, but they progressively shift towards clustering better with sparser networks as the network regresses until they eventually group with the *Rb* networks. The other arm of branch point (7) leads to a large grouping containing a set of well defined clusters. Branch point (8) splits off a small group with both *Rb* and *Pv* represented, but there is no clear common linkage. Conversely, branch point (9) yields a large group that is composed predominantly of *Pv* on black sand (with subgroups based on resource levels) and a few interspersed large networks, followed by a well-defined set of groups lying under branch point (10). The first cluster contains most of the *Pi* and *Pp* networks (although a few

such networks are located in the adjacent clusters), and the second cluster has sequential groups of *Pv* with high levels of resource but little grazing, a group with both grazing and species interaction, and a group with just species interaction.

It is not surprising that the structural and functional taxonomies both contain fine-grained complexity in their terminal groups, as several of the attributes have opposing effects that depend on the developmental age of each species and the combination of treatments. For example, as a fungal network grows, it tends to change from a branching tree to a more highly cross-linked network through hyphal and cord fusions that connect to each other. The core parts of a fungal network subsequently start to thin out as it explores further until resources run out; the network progressively recycles more cords and again becomes a very sparse network [1, 2].

Some of the clearest clusters in the PS-based taxonomy correlate with substrate, as there are distinct branches in the taxonomy that consist predominantly of *Pv* grown on black sand. Thus, even though *Pv* is well-represented in the dendrogram, there is a distinguishable effect of substrate on network architecture that is not immediately obvious to a human observer. Likewise, it is surprising that clear signatures are recovered in the PS dendrogram that correlate with resource level, grazing, and interactions with other species. Such observations underscore the fact that taxonomical groupings of fungal networks that are derived through network analysis can be of considerable assistance to biologists in their attempts to capture the impact of treatment combinations on network behaviour. The construction and analysis of network taxonomies also allow objective groupings of networks across species, treatments, and laboratory settings.

Constructing structural and functional taxonomies has the potential to be crucial for the development of increased understanding of subtle behavioural traits in biological networks. This type of approach should become more important as more networks are included in a classification — particularly if at least some have associated experimentally validated functional attributes [7–9]. Recently developed sophisticated network extraction algorithms [11] can dramatically improve the speed, accuracy, and level of detail of fungal networks. They also facilitate automated, high-throughput analysis of fungal network images, which can in turn be used to construct a richly detailed set of networks that are ripe for study via structural and functional network taxonomies.

S3. CONCLUSIONS

We calculated MRFs for a large set of networks of fungi and slime moulds. We considered two types of networks: (1) "structural" networks in which we calculate edge weights based on conductance values and (2) "functional" networks in which we calculate edge weights based on an estimate of how important edges are for the transport of nutrients. Calculating MRFs for the fungal and slime-mould networks in each of these two situations makes it possible to construct taxonomies and thereby compare large sets of fungal networks to each other. We illustrated that network taxonomies allow objective groupings of networks across species, treatments, and laboratories. The classification provides fine-grained structure that recovers the subtle interplay between species, substrate, resource level, grazing pressure, and inter-species competition. We also observed that networks undergoing major transitions, such as regressing from a fully connected meshwork to a sparse tree as resources run out, are dispersed across the tree. This reflects the shift in their functional behaviour amidst such transitions.

[1] Bebber, D., Hynes, J., Darrah, P. R., Boddy, L., & Fricker, M. D. (2007). Biological solutions to transport network design. *Proceedings of the Royal Society B: Biological Sciences*, **274**, 2307–2315.

[2] Boddy, L., Wood, J, Redman, E., Hynes, J., & Fricker, M. D. (2010). Fungal network responses to grazing. *Fungal Genetics and Biology*, **47**, 522–530.

[3] Buller, A. H. R. (1931). *Researches on fungi*, **4**. Longmans Green, London

[4] Csermely, P., London, A., Wu, L.-L., & Uzzi, B. (2013). Structure and dynamics of core/periphery networks. *Journal of Complex Networks*, **1**, 93–123.

[5] Fortunato, S. (2010). Community detection in graphs. *Physics Reports*, **486**, 75–174.

[6] Fricker, M. D., Boddy, L., Nakagaki, T., & Bebber, D. P. (2009). Adaptive biological networks. In Gross T. & Sayama H. (Eds.), *Adaptive Networks: Theory, Models and Applications* (pp. 51–70). Springer, New York, United States.

[7] Heaton, L. L. M., López, E., Maini P. K., Fricker M. D., & Jones, N. S. (2010). Growth-induced mass flows in fungal networks. *Proceedings of the Royal Society B: Biological Sciences*, **277**, 3265–3270.

[8] Heaton, L. L. M., Obara, B., Grau, V., Jones, N. S., Nakagaki, T., Boddy, L., & Fricker, M. D. (2012). Analysis of fungal networks. *Fungal Biology Reviews*, **26**, 12–29.

[9] Heaton, L. L. M., López, E., Maini, P. K., Fricker, M. D., & Jones, N. S. (2012). Advection, diffusion, and delivery over a network. *Physical Review E*, **86**, 021905.

[10] Katifori, E., Szöllősi, G. J., & Magnasco, M. O. (2010). Damage and fluctuations induce loops in optimal transport networks. *Physical Review Letters*, **104**, 048704.

[11] Obara, B., Garu, V., & Fricker, M. D. (2012). A bioimage informatics approach for extraction and analysis of fungal networks. *Bioinformatics*, **28**, 2374–2381.

[12] Lee, S. H., Cucuringu, M., & Porter, M. A. (2014). Density-based and transport-based core-periphery structures in networks. *Physical Review E*, **89**, 032810.

[13] Cucuringu, M., Rombach, M. P., Lee, S. H., & Porter, M. A. (2014). Detection of core-periphery structure in networks using spectral methods and geodesic paths. e-print arXiv:1410.6572.

[14] Newman, M. E. J. (2010). *Networks: an introduction* (Oxford University Press, UK).

[15] Onnela, J.-P., Fenn, D. J., Reid, S., Porter, M. A., Mucha, P. J., Fricker, M. D., & Jones, N. S. (2012). Taxonomies of networks

from community structure. *Physical Review E*, **86**, 036104.

[16] Porter, M. A., Onnela, J.-P., & Mucha, P. J. (2009). Communities in Networks. *Notices of the American Mathematical Society*, **56**, 1082–1097, 1164–1166.

[17] Reichardt, J., & Bornholdt, S. (2006). Statistical mechanics of community detection. *Physical Review E*, **74**, 016110.

[18] Tordoff, G.M., Boddy, L., & Jones, T.H. (2006). Grazing by Folsomia candida (Collembola) differentially affects mycelial morphology of the cord-forming basidiomycetes Hypholoma fasciculare, Phanerochaete velutina and Resinicium bicolor. *Mycological Research*, **110**, 335–345.

[19] Valente, T.W., & Fujimoto, K. (2010). Bridging: Locating critical connectors in a network. *Social Networks*, **32**, 212–220.